



# MIT Open Access Articles

## *Progress in fabrication of anisotropic Bragg gratings fabricated in lithium niobate via femtosecond laser micromachining*

The MIT Faculty has made this article openly available. **Please share** how this access benefits you. Your story matters.

<b>Citation</b>	Jolly, Sundeep, Savidis, Nickolaos, Datta, Bianca, Karydis, Thrasyvoulos, Langford, William et al. 2018. "Progress in fabrication of anisotropic Bragg gratings fabricated in lithium niobate via femtosecond laser micromachining."
<b>As Published</b>	10.1117/12.2289157
<b>Publisher</b>	SPIE
<b>Version</b>	Final published version
<b>Citable link</b>	<a href="https://hdl.handle.net/1721.1/137894">https://hdl.handle.net/1721.1/137894</a>
<b>Terms of Use</b>	Article is made available in accordance with the publisher's policy and may be subject to US copyright law. Please refer to the publisher's site for terms of use.

# PROCEEDINGS OF SPIE

[SPIDigitalLibrary.org/conference-proceedings-of-spie](https://spiedigitallibrary.org/conference-proceedings-of-spie)

## Progress in fabrication of anisotropic Bragg gratings fabricated in lithium niobate via femtosecond laser micromachining

Sundeeep Jolly, Nickolaos Savidis, Bianca Datta, Thrasyvoulos Karydis, Will Langford, et al.

Sundeeep Jolly, Nickolaos Savidis, Bianca Datta, Thrasyvoulos Karydis, Will Langford, Neil Gershenfeld, V. Michael Jr. Bove, "Progress in fabrication of anisotropic Bragg gratings fabricated in lithium niobate via femtosecond laser micromachining," Proc. SPIE 10544, Advanced Fabrication Technologies for Micro/Nano Optics and Photonics XI, 105440D (22 February 2018); doi: 10.1117/12.2289157

**SPIE.**

Event: SPIE OPTO, 2018, San Francisco, California, United States

# Progress in fabrication of anisotropic Bragg gratings in lithium niobate via femtosecond laser micromachining

Sundee Jolly<sup>a</sup>, Nickolaos Savidis<sup>a</sup>, Bianca Datta<sup>a</sup>, Thrasyvoulos Karydis<sup>b</sup>, Will Langford<sup>b</sup>, Neil Gershenfeld<sup>b</sup>, and V. Michael Bove, Jr.<sup>a</sup>

<sup>a</sup>MIT Media Lab, Massachusetts Institute of Technology, Cambridge, MA, United States

<sup>b</sup>Center for Bits and Atoms, Massachusetts Institute of Technology, Cambridge, MA, United States

## ABSTRACT

We have previously introduced a femtosecond laser micromachining-based scheme for the fabrication of anisotropic waveguides and isotropic Bragg reflection gratings in lithium niobate for application in future integrated-optic spatial light modulators. In this paper, we depict progress in fabrication and characterization of anisotropic Bragg reflection gratings fabricated in lithium niobate via Type I femtosecond laser-based permittivity modulation. We furthermore depict an electromagnetic analysis of such multilayer grating structures based around coupled-wave theory for thick holographic gratings.

**Keywords:** holography, near-to-eye display, waveguide optics

## 1. INTRODUCTION

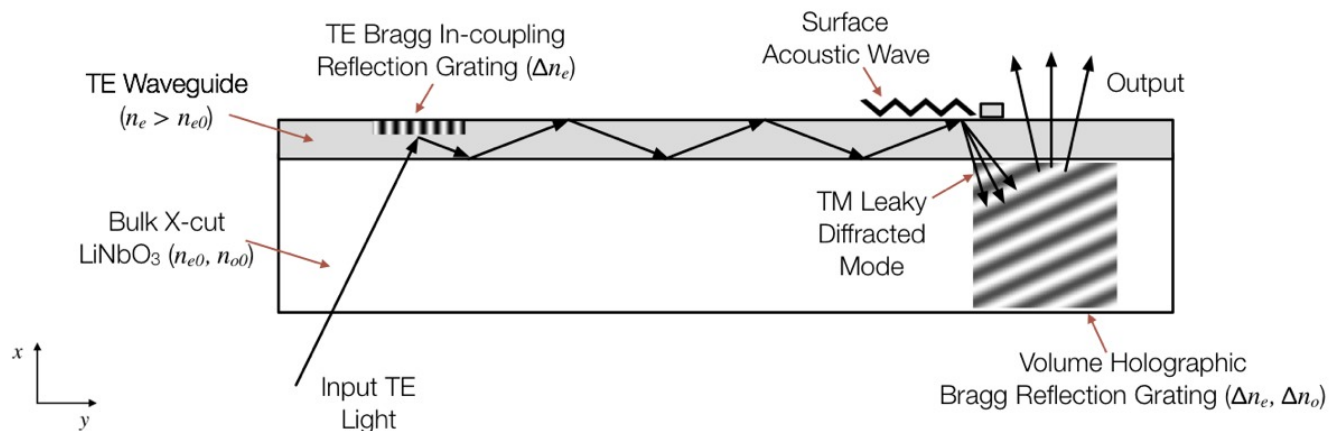


Figure 1.  $x - y$  cross-section (side view) of proposed guided optical wave SAW device with integrated Bragg gratings.

Lithium niobate ( $\text{LiNbO}_3$ ) is an important synthetic crystalline material widely used for applications in integrated and non-linear optics. Traditional processing schemes for the generation of integrated photonic structures within  $\text{LiNbO}_3$  substrates have typically included conventional resist-based photolithographic and electron-beam lithographic techniques alongside wet-<sup>1</sup> or dry-etching.<sup>2</sup> Furthermore, ion-diffusion techniques such as titanium indiffusion<sup>3</sup> and proton exchange<sup>4</sup> have yielded waveguide structures to great utility for the generation of active integrated acousto-optical<sup>5</sup> and electro-optical<sup>6</sup> devices.

Recently, direct laser writing has emerged as a promising alternative for the generation of embedded passive and active photonic structures within various optically transparent media.<sup>7</sup> The use of femtosecond laser micromachining in  $\text{LiNbO}_3$  has recently been proposed for fabrication of index-structures including waveguides,<sup>8-10</sup> multiplexing and de-multiplexing architectures,<sup>11</sup> diffraction gratings,<sup>12-15</sup> active metal layers, and volume holographic elements.

Corresponding author: [sjolly@media.mit.edu](mailto:sjolly@media.mit.edu)

We have previously proposed an active guided-wave acousto-optic device implemented in  $\text{LiNbO}_3$  for spatial light modulation in holographic display applications.<sup>16,17</sup> Structurally, our spatial light modulation solution (depicted in Fig. 1) is comprised of an anisotropic waveguide on a lithium niobate substrate. Guided optical modes interact with surface acoustic waves containing holographic information launched from the RF transducer and are thereby rotated in polarization and outcoupled from the waveguide. Finally, the modulated light is incident on a reflection volume grating which acts to steer the modulated output towards a viewer. We have previously depicted a fabrication methodology for such a device based on femtosecond laser micromachining of waveguides.<sup>18,19</sup> In this paper, we depict progress in fabrication of volume Bragg gratings in lithium niobate for application in light outcoupling via femtosecond laser micromachining.

## 2. FEMTOSECOND LASER MICROMACHINING IN LITHIUM NIOBATE

Femtosecond laser structuring of transparent media is widely used to create 2-D and 3-D profiles in refractive index within the volume of said media,<sup>7</sup> subject to limitations imposed on resolution and achievable modulation by the diffraction-limited waist size of the focusing objective and material thresholds for densification and available dynamic range. Previous studies of femtosecond laser micromachining in lithium niobate have focused on the integration of embedded photonic structures on the surface or within the volume of the crystalline substrate, usually by means of a permanent change of birefringent refractive index via lattice densification,<sup>10</sup> although techniques exploiting volumetric photorefractive modifications have also been utilized.<sup>20</sup>

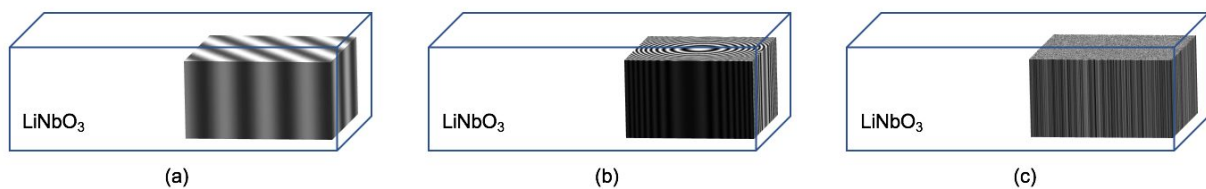


Figure 2. Volumetric grating structures achievable in  $\text{LiNbO}_3$  via femtosecond laser processing. (a) Volume Bragg gratings having arbitrary fringe geometries, (b) Volume Bragg gratings having optical power (e.g., spherical-beam or cylindrical-beam volume holograms), (c) Aperiodic optical structures having arbitrary modulation of refractive index at each voxel location.

Permanent refractive index modulation via densification in lithium niobate is often classified into two types of modifications: Type I, in which the extraordinary index is decreased but the ordinary index is unchanged via a femtosecond pulse train, and Type II, in which both uniaxial indices are decreased via a pulse train with pulse durations over 1 ps.<sup>9</sup> Previous studies have indicated the feasibility of fabricating Raman-Nath and volume Bragg gratings in  $\text{LiNbO}_3$ .<sup>13–15</sup> Although volumetric grating structures are achievable via photorefractive recording in  $\text{LiNbO}_3$ , the recording of arbitrary fringe geometries in angle and periodicity is often cumbersome due to the sometimes extreme propagation angles required of either beam in two-beam holographic recording. In contrast to optical holographic recording, femtosecond laser micromachining offers the ability to embed arbitrary fringe geometries without the need to adjust optical paths for two-beam interference, diffractive lenses having optical power, photonic crystal structures, or completely aperiodic volumetric structures in refractive index (see Fig. 2). Here, we depict volumetric grating designs applicable for use in guided-wave acousto-optic devices and describe current progress in their fabrication via femtosecond laser micromachining.

### 3. VOLUME GRATING DESIGN AND ANALYSIS

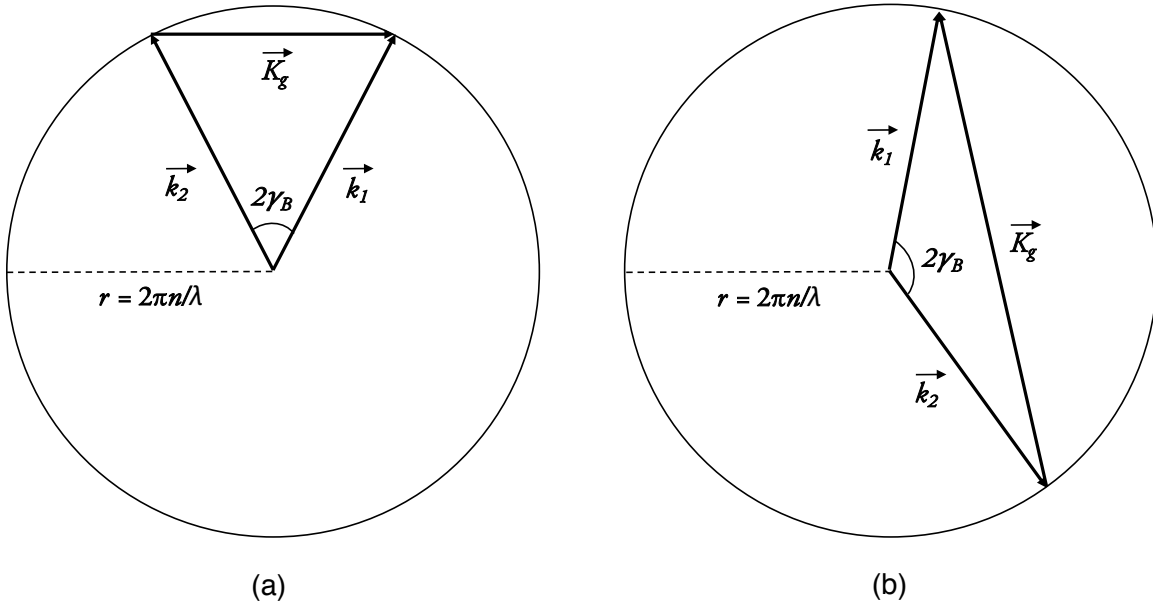


Figure 3. Conservation of momentum in Bragg (a) transmission and (b) reflection gratings.  $\vec{K}_g$  is the recorded grating vector,  $\vec{k}_2$  is the output wavevector,  $\vec{k}_1$  is the input wavevector, and  $\gamma_B$  is the Bragg angle of the recorded grating.

The fabrication of a volume Bragg grating with desired diffractive behavior is dependent on the grating vector  $\vec{K}_g$  that dictates the input and output beams. This relationship is depicted on the Descartes sphere (shown in 2-D for simplicity) for transmission and reflection volume holographic gratings in Fig. 3. Due to conservation of momentum, the relationship  $\vec{K}_g = \vec{k}_2 - \vec{k}_1$  dictates the diffracted output wavevector  $\vec{k}_1$  for a given Bragg-matched input wavevector  $\vec{k}_2$  and grating vector  $\vec{K}_g$ . From a geometrical perspective, the Bragg angle can be backcalculated from the grating period for a given illumination wavelength as  $\gamma_B = \sin^{-1}(\lambda/2\Lambda)$ .

According to Kogelnik's coupled-wave theory,<sup>21-23</sup> we present several analyses of the the influence of overall grating thickness on device performance in both transmission and reflection geometries (Figs. 4 and 5) for LiNbO<sub>3</sub> with an average unmodulated refractive index  $n_{av} = 2.28$  and assuming a maximal achievable femtosecond laser-induced index modulation of  $\Delta n = 5 \times 10^{-4}$  (as is consistent with bounds reported in the literature<sup>9,10</sup>). Figs. 4 and 5 depict the influence of the angular incidence relative to the fully Bragg-matched condition on diffraction efficiency for transmission and reflection volume gratings, respectively. For femtosecond laser micromachined gratings in LiNbO<sub>3</sub>, the effect of the number of grating layers (having axial thickness of 5  $\mu\text{m}$ ) on the diffraction efficiency of the reflection grating is depicted in Fig. 6. Note that the axial thickness used for this simulated result is consistent with those expected with typical objectives used in our experimental setup, depicted in the following section.

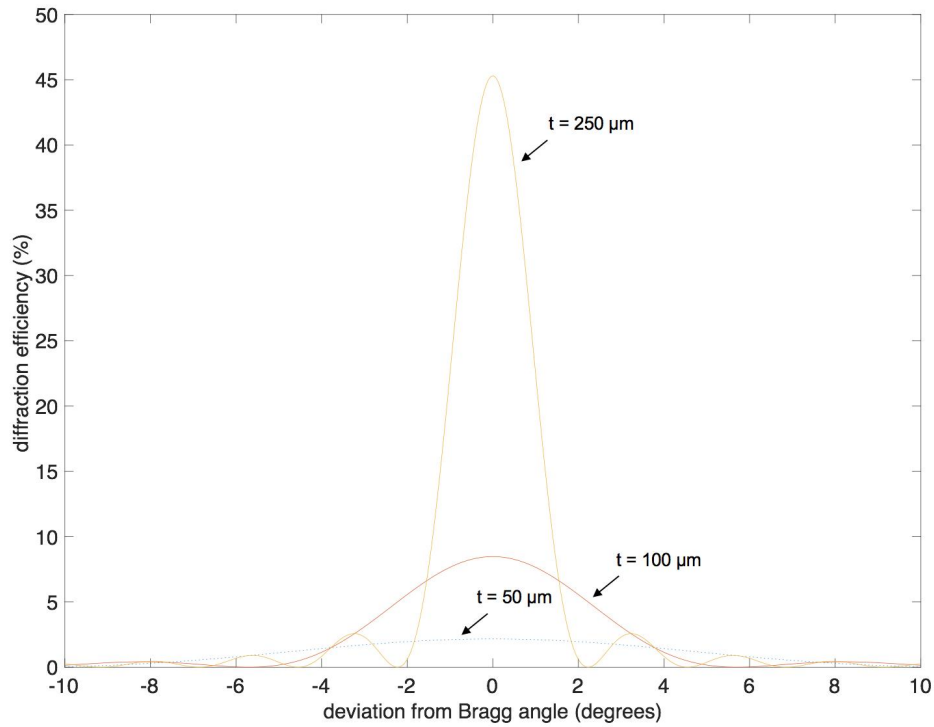


Figure 4. Diffraction efficiency for an unslanted volume transmission grating with  $\Lambda = 10 \mu\text{m}$  as a function of Bragg mismatch angle for  $\lambda = 532 \text{ nm}$  illumination and  $t = 50 \mu\text{m}$ ,  $t = 100 \mu\text{m}$ , and  $t = 250 \mu\text{m}$ .

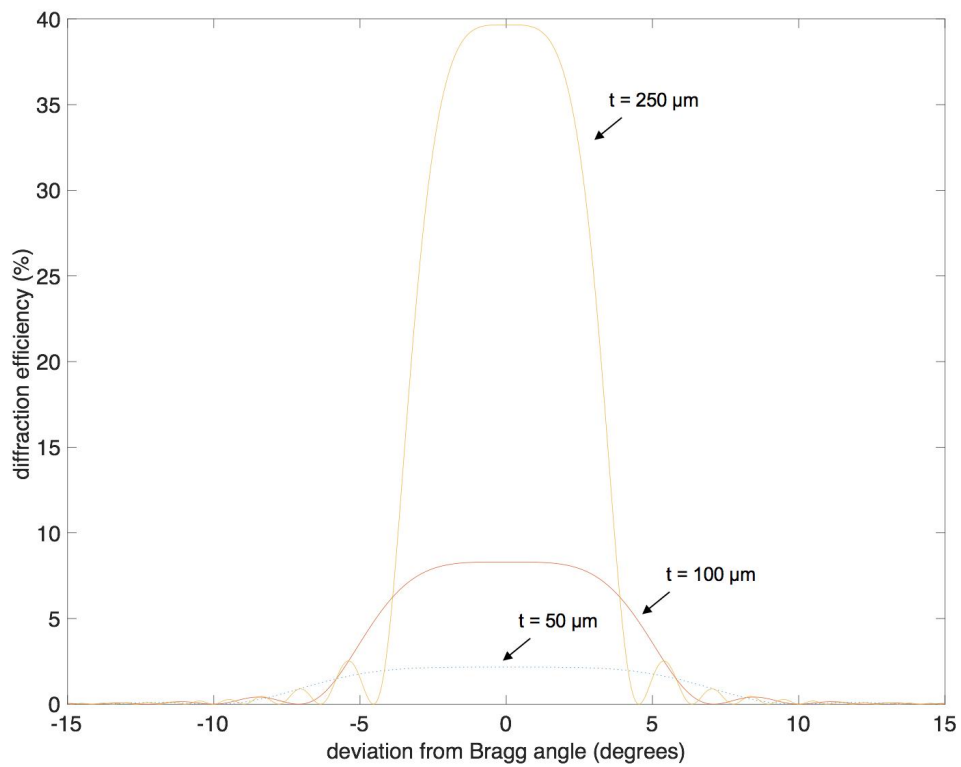


Figure 5. Diffraction efficiency for an unslanted volume reflection grating with  $\Lambda = 10 \mu\text{m}$  as a function of Bragg mismatch angle for  $\lambda = 532 \text{ nm}$  illumination and  $t = 50 \mu\text{m}$ ,  $t = 100 \mu\text{m}$ , and  $t = 250 \mu\text{m}$ .

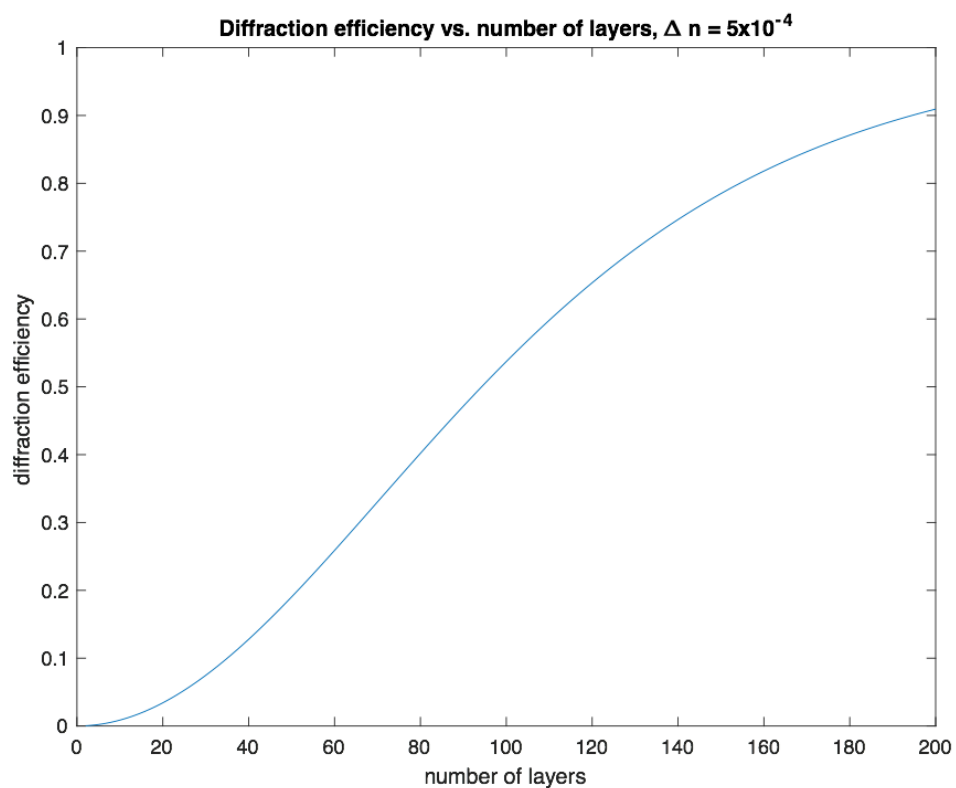


Figure 6. Influence of number of micromachined grating layers on diffraction efficiency for an unslanted volume reflection grating with  $\Lambda = 10 \mu\text{m}$  and for  $\lambda = 532 \text{ nm}$  illumination, assuming a  $5 \mu\text{m}$  axial resolution in the writing spot.

#### 4. EXPERIMENTAL METHODOLOGY

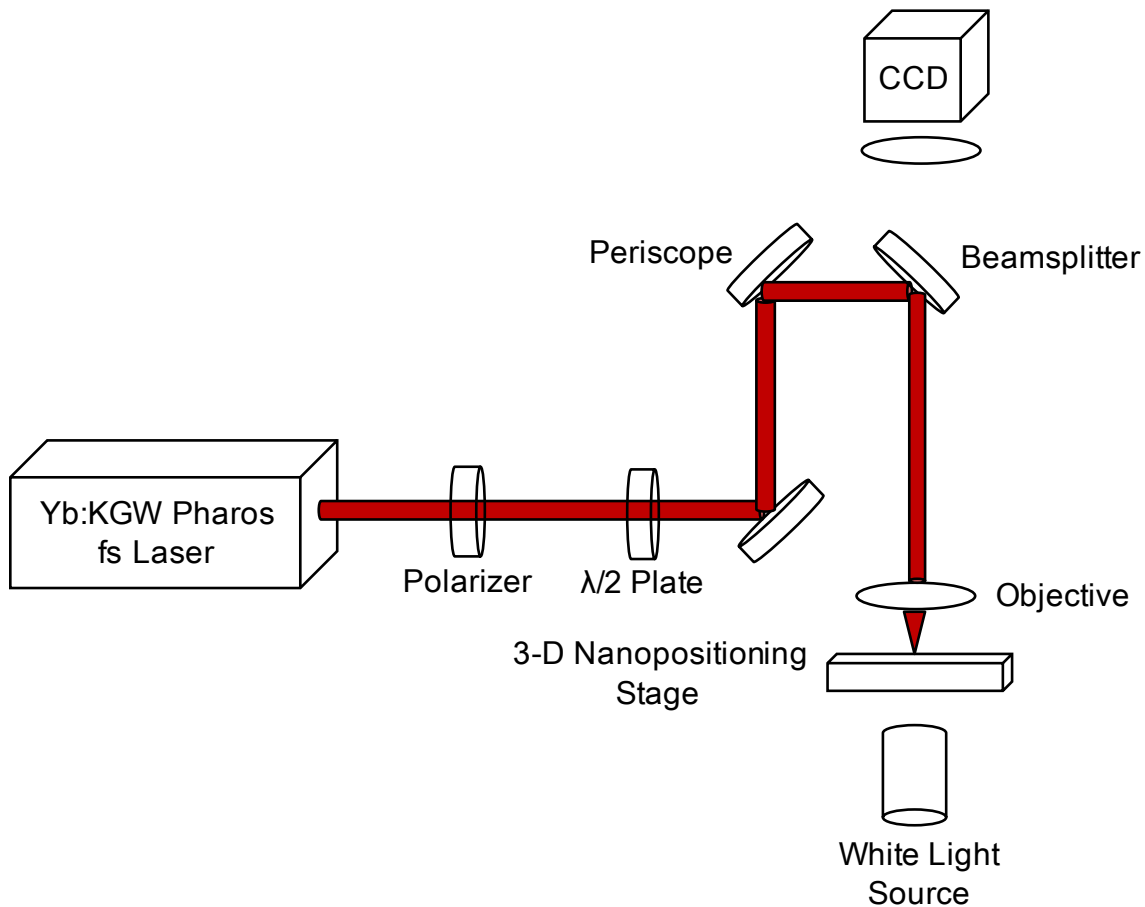


Figure 7. Setup schematic for femtosecond laser micromachining.

The setup presented here for femtosecond laser micromachining is depicted in Fig. 7. A femtosecond beam from a Yb:KGW femtosecond laser source (Light Conversion Pharos 15W, fundamental operating wavelength  $\lambda = 1030$  nm with available harmonics at  $\lambda = 515$  nm and  $\lambda = 343$  nm) is input to a polarizer and  $\lambda/2$  plate for control of beam attenuation. The beam is input to a periscope and reflected off a beamsplitter into the entrance pupil of a microscope objective (Mitutoyo 10X NA=0.28 infinity-corrected plan apochromatic) that acts to focus the beam into the volume of the LiNbO<sub>3</sub> substrate. The sample is mounted on a computer-controlled 3-axis nanopositioning stage (SmarAct, GMBH) with 1 nm resolution and high repeatability. To control the grating exposure, interfaces to both the laser and stage are controlled via custom software that triggers the beam on while the stage is moving along the axis of a grating finger to be written, off while the stage translates between grating fingers.

A white light source is added underneath the transparent sample in order to use the objective along with a CCD camera for imaging simultaneously with writing within the medium with the femtosecond beam. This setup is depicted in Fig. 8.

For the purposes of the current experiment, we use x-cut LiNbO<sub>3</sub> wafers with thickness of 1 mm. We use the femtosecond laser source with an operating wavelength at the fundamental  $\lambda = 1030$  nm, repetition rate of 100 kHz, a 2  $\mu$ J pulse energy, and with the stage translating at 2.5 mm/s while writing any particular grating finger. In all results presented here, the grating fingers are parallel to the LiNbO<sub>3</sub> *c*-axis.



Figure 8. Setup for femtosecond laser micromachining.

## 5. EXPERIMENTAL RESULTS, PROJECT STATUS, AND FUTURE WORK

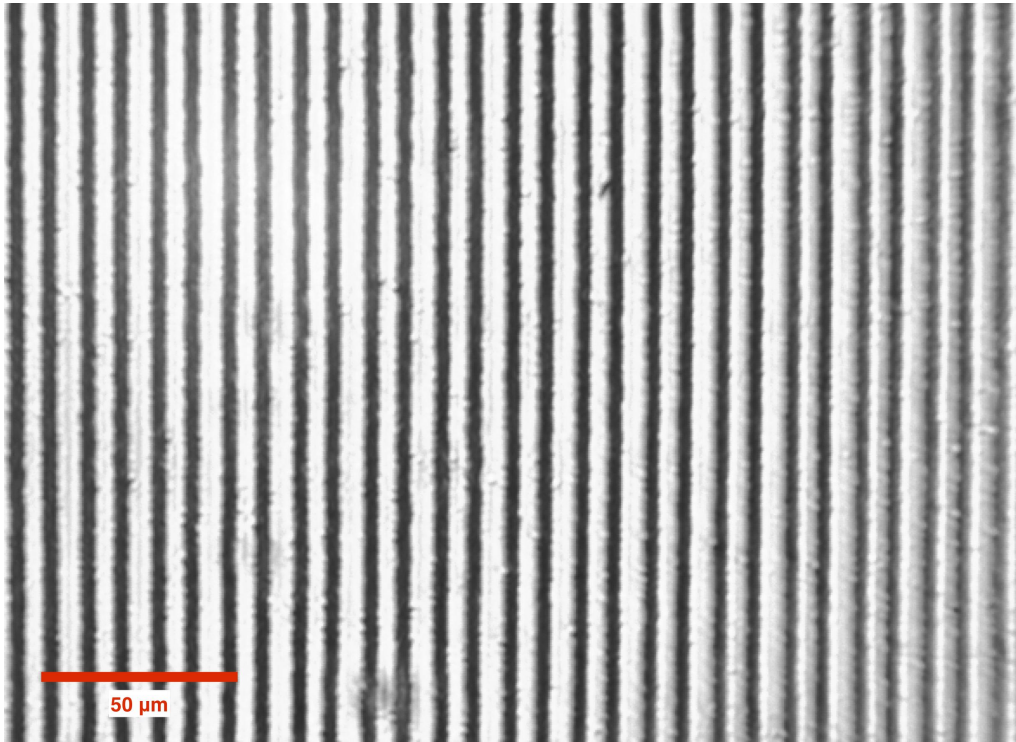


Figure 9. Optical micrograph of surface grating with  $\Lambda = 10 \mu\text{m}$  fabricated on  $\text{LiNbO}_3$  surface.

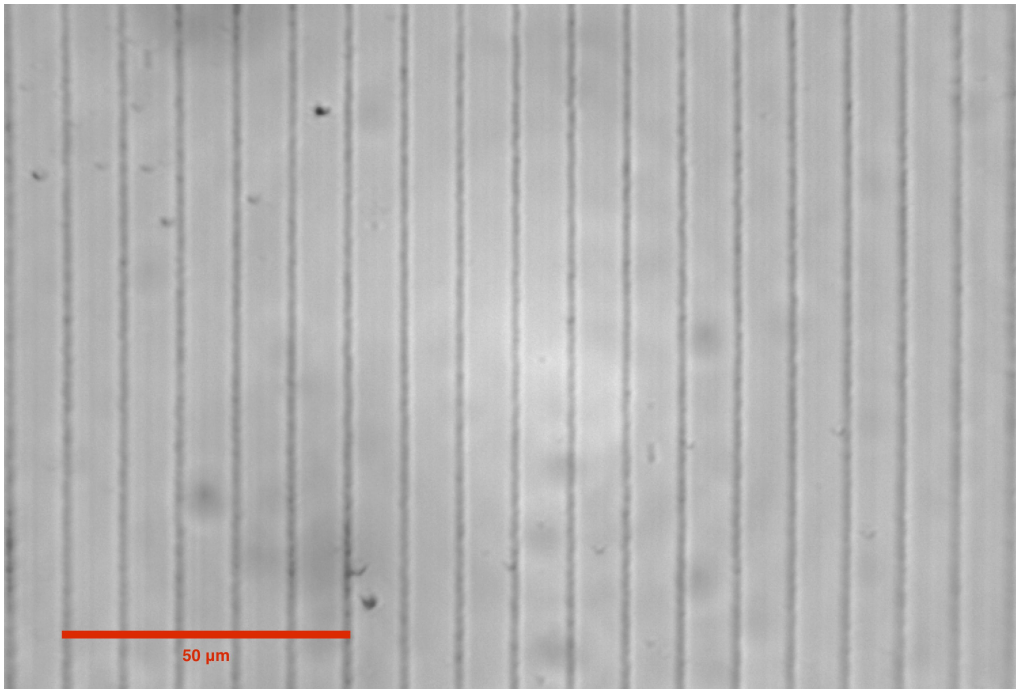


Figure 10. Optical micrograph of volume phase grating with  $\Lambda = 10 \mu\text{m}$  and thickness  $t = 50 \mu\text{m}$  fabricated  $150 \mu\text{m}$  below the  $\text{LiNbO}_3$  surface.



Figure 11. Diffracted output from volume phase grating.

At the time of this writing, we have successfully fabricated simple surface and volume transmission gratings in lithium niobate. Fig. 9 depicts an optical micrograph of a surface grating with  $\Lambda = 10 \mu\text{m}$  and Fig. 10 depicts the top surface of a volume transmission phase grating with  $\Lambda = 10 \mu\text{m}$  and thickness  $t = 50 \mu\text{m}$  fabricated  $150 \mu\text{m}$  below the  $\text{LiNbO}_3$  surface, with layer thickness chosen to be  $5 \mu\text{m}$  to correspond to a longer axial spot size. The  $1/e^2$  lateral spot size emerging at the focus of the objective is measured to be  $2.5 \mu\text{m}$ . Fig. 10 depicts the diffracted output from the volume phase grating when illuminated at the Bragg angle  $\gamma_B = 1.5^\circ$ . At the time of this writing, we have not yet observed anisotropic effects due to the polarization of the probe beam incident on the direct-written grating.

Future work on this effort will include characterization and optimization of the anisotropy of the written gratings, further optimization for diffraction efficiency, fabrication of reflection geometry volume Bragg gratings, and an analysis of the multilayered phase grating structure via a computational electromagnetic method.<sup>24</sup>

## ACKNOWLEDGEMENTS

This research has been supported by consortium funding at the MIT Media Laboratory and by Air Force Research Laboratory contract FA8650-14-C-6571. The authors gratefully acknowledge facility use and technical assistance by the MIT Nanostructures Laboratory and the MIT Center for Bits and Atoms.

## REFERENCES

- [1] Hu, H., Ricken, R., Sohler, W., and Wehrspohn, R. B., "Lithium Niobate Ridge Waveguides Fabricated by Wet Etching," *IEEE Photonics Technology Letters*, 19(6), 417-419 (2007).
- [2] Tamura, M. and Yoshikado, S., "Etching characteristics of  $\text{LiNbO}_3$  crystal by fluorine gas plasma reactive ion etching," *Surface and Coatings Technology*, 169, 203-207 (2003).
- [3] Turner, E. H., Alferness, R. C., and Schmidt, R. V., "Characteristics of Ti-diffused lithium niobate optical directional couplers," *Applied Optics*, 18(23), 4012-4016 (1979).
- [4] Rice, C. E. and Jackel, J. L., "Structural changes with composition and temperature in rhombohedral  $\text{Li}_{1-x}\text{H}_x\text{NbO}_3$ ," *Materials Research Bulletin*, 19(5), 591-597 (1984).
- [5] Hinkov, V., "Proton exchanged waveguides for surface acoustic waves on  $\text{LiNbO}_3$ ," *Journal of Applied Physics*, 62(9), 3573-3578 (1998).
- [6] Noviello, G., Armenise, M. N., and Passaro, V. M. N., "Lithium niobate guided-wave beam former for steering phased-array antennas," *Applied Optics*, 33(26), 6194-6209 (1994).
- [7] Gattass, R. R. and Mazur, E., "Femtosecond laser micromachining in transparent materials," *Nature Photonics*, 2(4), 219-225 (2008).

- [8] Bookey, H. T., Thomson, R. R., Psaila, N. D., Kar, A. K., Chiodo, N., Osellame, R., and Cerullo, G., "Femtosecond Laser Inscription of Low Insertion Loss Waveguides in Z-Cut Lithium Niobate," *IEEE Photonics Technology Letters*, 19(12), 892-894 (2007).
- [9] Burghoff, J., Nolte, S., and Tunnermann, A., "Origins of waveguiding in femtosecond laser-structured LiNbO<sub>3</sub>," *Applied Physics A*, 89(1), 127-132 (2007).
- [10] Burghoff, J., Hartung, H., Nolte, S., and Tunnermann, A., "Structural properties of femtosecond laser-induced modifications in LiNbO<sub>3</sub>," *Applied Physics A*, 86(2), 165-170 (2007).
- [11] Thomas, J., Heinrich, M., Zeil, P., Hilbert, V., Rademaker, K., Riedel, R., Ringleb, S., Dubs, C., Ruske, J. P., Nolte, S. and Tannermann, A. "Laser direct writing: Enabling monolithic and hybrid integrated solutions on the lithium niobate platform," *Physica Status Solidi (a)*, 208(2), 276-283 (2011).
- [12] Beresna, M. and Kazansky, P. G., "Polarization diffraction grating produced by femtosecond laser nanostructuring in glass," *Optics Letters*, 35(10), 1662-1664 (2010).
- [13] Denz, C., Herrmann, J., Imbrock, J., Kroesen, S., and Horn, W., "Electro-optical tunable waveguide Bragg gratings in lithium niobate induced by femtosecond laser writing," *Optics Express*, 20(24), 26922-26928 (2012).
- [14] Dietrich, C., Denz, C., Imbrock, J., Kroesen, S., and Horn, W., "Femtosecond Laser-Induced Volume Gratings in Lithium Niobate for Noncollinear Second-Harmonic Generation," *Proceedings of CLEO 2014* (2014).
- [15] Paipulas, D., Kudriaov, V., Malinauskas, M., Smilgevicius, V., and Sirutkaitis, V., "Diffraction grating fabrication in lithium niobate and KDP crystals with femtosecond laser pulses," *Applied Physics A*, 104(3), 769-773 (2011).
- [16] Smalley, D. E., Smithwick, Q. Y. J., Bove, V. M., Barabas, J. and Jolly, S. "Anisotropic leaky-mode modulator for holographic video displays," *Nature* 498, 313-317 (2013).
- [17] Jolly, S., Savidis, N., Datta, B., Smalley, D. E., and Bove, V. M., "Near-to-eye electroholography via guided-wave acousto-optics for augmented reality," *Proc. SPIE 10127* (2017).
- [18] Savidis, N., Jolly, S., Datta, B., Karydis, T., and Bove, V. M., "Fabrication of waveguide spatial light modulators via femtosecond laser micromachining," *Proc. SPIE 9759*, 97590R12 (2016).
- [19] Savidis, N., Jolly, S., Datta, B., Moebius, M., Karydis, T., Mazur, E., Gershenfeld, N., and Bove, V. M., "Progress in fabrication of waveguide spatial light modulators via femtosecond laser micromachining," *Proc. SPIE 10115* (2017).
- [20] Paipulas, D., Mizeikis, V., Purlys, V., Cerkauskaitė, A., and Juodkazis, S., "Volumetric integration of photorefractive micromodifications in lithium niobate with femtosecond laser pulses," *Proc. SPIE 9374*, 93740B-13 (2015).
- [21] Kogelnik, H., "Coupled wave theory for thick hologram gratings," *The Bell System Technical Journal* (1969).
- [22] Ciapurin, I. V., Glebov, L. B. and Smirnov, V. I., "Modeling of Gaussian beam diffraction on volume Bragg gratings in PTR glass," *Proc. SPIE 5742*, 183-194 (2005).
- [23] Ciapurin, I. V., Drachenberg, D. R., Smirnov, V. I., Venus, G. B. and Glebov, L. B. "Modeling of phase volume diffractive gratings, part 2: reflecting sinusoidal uniform gratings, Bragg mirrors," *Optical Engineering*, 51(5) (2012).
- [24] Lee, W. and Degertekin, F. L., "Rigorous coupled-wave analysis of multilayered grating structures," *Journal of Light-wave Technology*, 22(10) (2004).